

STUDY OF A TRAVELING COMBUSTION FRONT ON A PETROLEUM BED MODEL

U. P. Kuvanyshv and R. L. Nasibullin

UDC 536.46:622.276

Results are shown of an experimental study concerning the combustion process inside a petroleum bed and the mathematical description of the temperature field in a tubular model of such a bed. The test data are compared with calculated values.

A traveling combustion front for the extraction of petroleum under laboratory conditions is produced most often in circular steel tubes filled with oil-bearing sandstone and equipped with igniting, insulating, and measuring devices [2, 3].

Tests were performed with an apparatus shown in Fig. 1. The bed model consisted of two coaxial tubes: an inner one 100 mm in diameter and an outer one 240 mm in diameter. The inner tube served as a shell to confine the oil-bearing sandstone and the outer tube served to retain the asbestos insulation. The total length of the model was 1200 mm. Eleven thermocouple wells spaced 120 mm apart were installed along the model for temperature measurements.

After the permeability of the porous medium had been determined, the electric igniter and the inlet segment of the model tube were heated up to a 350-370°C temperature. Then, air from the tank was injected into the bed model under a 1-3 atm pressure. When the inlet temperature increased rapidly, as indicated by an oil flame, the electric heater was switched off.

The combustion process was monitored by thermocouple readings as well as by the CO₂ and O₂ contents in the flue gas. The process was controlled by regulating the air supply pressure. As the combustion front was progressing, gaseous products together with water, vapor, and oil were escaping from the model. We will show here the initial data and the results of one such test performed with high-viscosity oil from Tatar deposits (sandstone porosity 38.5%, permeability 1.56 darcy, oil saturation level 26.8% of the pores volume, water saturation level 14.2% of the pores volume, air flow rate 0.408 Nm³/h, mean velocity of combustion front 0.15 m/h, temperature at the combustion front 654°C, sandstone density 1640 kg/m³, combustible fraction of oil 48 kg per 1 m³ of sandstone, interstitial air flow density 566 Nm³ per 1 m³ of sandstone, flue gas composition: 3.64% O₂, 10.39% CO₂, and 4.8% CO; oxygen utilization factor 81.1%, oil extraction factor 57.5%).

In order to describe the temperature field, we make the following assumptions: that the combustion front at a given thermal power (unlike at a given temperature, as in [3]) travels at a constant velocity while the air flow rate remains constant; that the temperature is uniform across a radial section; that the heat losses into the surrounding medium are subject to Newton's law of heat transmission; that the thickness of the combustion front is negligibly small; that the heat is transferred along the tube axis by the traveling front, by convection, and by conduction; that the thermophysical properties of the system are not temperature-dependent; and that the heat transfer between sand grains and fluids impregnating them occurs instantaneously.

Based on the heat balance for this tube under such conditions, we obtain the following differential equation for determining the temperature:

$$\frac{\partial^2 T}{\partial x^2} - \frac{\rho_a c_a u}{\lambda} \cdot \frac{\partial T}{\partial x} - \frac{2k}{\lambda R} (T - T_0) = \frac{1}{\gamma} \cdot \frac{\partial T}{\partial t} - \frac{u \rho_a N_0 g}{\lambda} \delta(x - vt) \quad (1)$$

Tatar State Scientific-Research and Design Institute of the Petroleum Industry, Bugul'ma. Translated from *Inzhenerno-Fizicheskii Zhurnal*, Vol. 22, No. 3, pp. 488-493, March, 1972. Original article submitted March 16, 1971.

© 1974 Consultants Bureau, a division of Plenum Publishing Corporation, 227 West 17th Street, New York, N. Y. 10011. No part of this publication may be reproduced, stored in a retrieval system, or transmitted, in any form or by any means, electronic, mechanical, photocopying, microfilming, recording or otherwise, without written permission of the publisher. A copy of this article is available from the publisher for \$15.00.

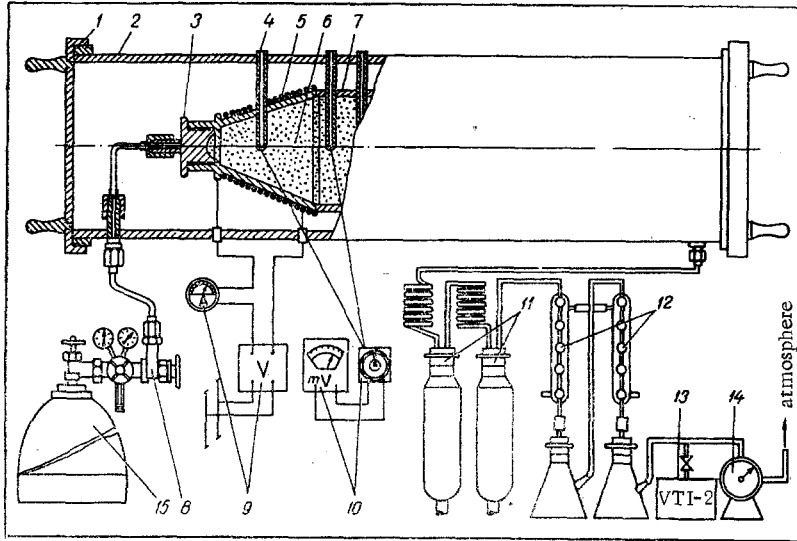


Fig. 1. Schematic diagram of the laboratory apparatus for studying the combustion of petroleum in a tube: (1) lid, (2) jacket, (3) stopper, (4) thermocouple well, (5) electric heater, (6) oil-bearing sandstone, (7) model shell (combustion tube), (8) air throttle, (9) checking and measuring instruments for the electric heater, (10) electrothermometer, (11) and (12) separators, (13) gas analyzer, (14) gas counter, (15) compressed-air tank.

with the following initial and boundary conditions:

$$\begin{aligned} T &= T_m \exp(-bx) + T_0 & \text{at } t = 0, \\ T &= T_s & \text{at } x = 0, \quad T = T_0 & \text{at } x \rightarrow \infty. \end{aligned} \quad (2)$$

We now introduce the dimensionless parameters

$$\begin{aligned} \bar{T} &= (T - T_0)/(T_s - T_0), \quad \bar{x} = x\rho_a c_a u/\lambda, \quad \bar{t} = tu^2 \rho_a^2 c_a^2 / \lambda c_{3s} \rho_s, \\ a &= 2k/Ru^2 \rho_a^2 c_a^2, \quad \kappa = v\rho_s c_s / uc_a \rho_a, \quad A = N_0 g / (T_s - T_0) c_a, \\ b_1 &= b\lambda / u\rho_a c_a \end{aligned}$$

and write Eq. (1) accordingly:

$$\frac{\partial^2 \bar{T}}{\partial \bar{x}^2} - \frac{\partial \bar{T}}{\partial \bar{x}} - a\bar{T} = \frac{\partial \bar{T}}{\partial \bar{t}} - \frac{A}{\kappa} \delta\left(\bar{t} - \frac{\bar{x}}{\kappa}\right). \quad (3)$$

Equation (3) together with conditions (2) is solved by the Laplace operational method [1]. Omitting all intermediate steps, we will show only the final solution for the temperature in the bed model:

$$\begin{aligned} T - T_0 &= \frac{1}{2} (T_s - T_0) \left[\exp\left(-\bar{x} \sqrt{\frac{1}{4} + a}\right) \operatorname{erfc}\left(\frac{\bar{x}}{2\sqrt{\bar{t}}}\right) \right. \\ &\quad \left. - \sqrt{\left(\frac{1}{4} + a\right)\bar{t}} + \exp\left(\bar{x} \sqrt{\frac{1}{4} + a}\right) \operatorname{erfc}\left(\frac{\bar{x}}{2\sqrt{\bar{t}}}\right) \right. \\ &\quad \left. + \sqrt{\left(\frac{1}{4} + a\right)\bar{t}} \right] + \frac{N_0 g}{c_a v (1 - \kappa)^2 + 4a} \left\{ e^{\bar{x}/2} \left[\frac{e^{\omega \bar{t}}}{2} \right. \right. \\ &\quad \left. \left. \times \left\{ \exp\left[-\bar{x} \sqrt{\frac{1}{4} + a + \omega_1}\right] \operatorname{erfc}\left[\frac{\bar{x}}{2\sqrt{\bar{t}}}\right] - \sqrt{\left(\frac{1}{4} + a + \omega_1\right)\bar{t}} \right] \right. \right. \\ &\quad \left. \left. + \exp\left[\bar{x} \sqrt{\frac{1}{4} + a + \omega_1}\right] \operatorname{erfc}\left[\frac{\bar{x}}{2\sqrt{\bar{t}}}\right] + \sqrt{\left(\frac{1}{4} + a + \omega_1\right)\bar{t}} \right] \right\} \end{aligned}$$

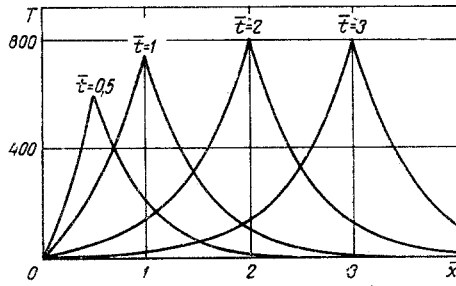


Fig. 2

Fig. 2. Transient temperature distribution (°C) as a function of the dimensionless distance and time, according to formula (4) with $a = 3.25$ and $\kappa = 1$.

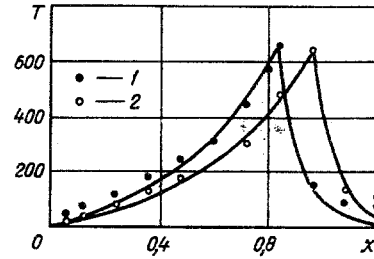


Fig. 3

Fig. 3. Comparison between measured temperatures of the bed model (°C) with the values calculated according to formula (9): test values 5.6 h (1) and 6.4 h (2) after the start of combustion. Distance x (m).

$$\begin{aligned}
 & -\frac{e^{\omega_2 \bar{t}}}{2} \left\{ \exp \left[-\bar{x} \sqrt{\frac{1}{4} + a + \omega_2} \right] \operatorname{erfc} \left[\frac{\bar{x}}{2\sqrt{\bar{t}}} - \sqrt{\left(\frac{1}{4} + a + \omega_2 \right) \bar{t}} \right] \right. \\
 & \quad \left. + \exp \left[\bar{x} \sqrt{\frac{1}{4} + a + \omega_2} \right] \operatorname{erfc} \left[\frac{\bar{x}}{2\sqrt{\bar{t}}} + \sqrt{\left(\frac{1}{4} + a + \omega_2 \right) \bar{t}} \right] \right\} \\
 & \quad + \left[\exp \omega_2 \left(\bar{t} - \frac{\bar{x}}{\kappa} \right) - \exp \omega_1 \left(\bar{t} - \frac{\bar{x}}{\kappa} \right) \right] U \left(\bar{t} - \frac{\bar{x}}{\kappa} \right) \\
 & \quad + T_m e^{-(a-b_1-b_1^2)\bar{t}} \left\{ e^{-b_1 \bar{t}} - \frac{e^{\bar{x}^2/2}}{2} \left\{ \exp \left(-\bar{x} \sqrt{\frac{1}{4} + b_1 + b_1^2} \right) \right. \right. \\
 & \quad \times \operatorname{erfc} \left[\frac{\bar{x}}{2\sqrt{\bar{t}}} - \sqrt{\left(\frac{1}{4} + b_1 + b_1^2 \right) \bar{t}} \right] + \exp \left[\bar{x} \sqrt{\frac{1}{4} + b_1 + b_1^2} \right] \\
 & \quad \left. \left. \times \operatorname{erfc} \left[\frac{\bar{x}}{2\sqrt{\bar{t}}} + \sqrt{\left(\frac{1}{4} + b_1 + b_1^2 \right) \bar{t}} \right] \right\} \right\}, \tag{4}
 \end{aligned}$$

where

$$\omega_1 = \frac{\kappa}{2} [\kappa - 1 + \sqrt{(1-\kappa)^2 + 4a}], \quad \omega_2 = \frac{\kappa}{2} [\kappa - 1 - \sqrt{(1-\kappa)^2 + 4a}].$$

The transient temperature distributions in a linear bed shown in Fig. 2 have been calculated according to solution (4) with $a = 3.25$, $\kappa = 1$, and $N_0g/c_a = 3000^\circ\text{C}$. The preheating of the bed has been disregarded in these calculations, i.e., $T_m = 0$ here and the pumped air has been assumed to be at atmospheric temperatures ($T_S = T_0$).

The calculations show that a temperature profile in the bed at $\bar{t} > 3$ becomes steady and is determined by the location of the combustion front. This is confirmed also to be the experimental temperature curves.

The steady-state solution is obtained from (4) by letting the diffusivity in this equation ($\gamma = \lambda/c_S\rho_S$) become infinite:

$$\begin{aligned}
 T - T_0 &= (T_S - T_0) \exp \left[-\frac{\bar{x}}{2} (-1 + \sqrt{1 + 4a}) \right] \\
 &+ \frac{N_0g}{c_a(1+4a)} \left\{ \exp \left[\frac{1}{2} (1 - \sqrt{1+4a})(\bar{x} - \kappa\bar{t}) \right] - \exp \frac{1}{2} [(\bar{x} - \kappa\bar{t}) \right. \\
 &\quad \left. - (\bar{x} + \kappa\bar{t}) \sqrt{1+4a}] - \left[\exp \left[-\frac{1}{2} (\kappa\bar{t} + \bar{x})(1 - \sqrt{1+4a}) \right] \right. \right. \\
 &\quad \left. \left. - \exp \left[-\frac{1}{2} (\kappa\bar{t} - \bar{x})(1 + \sqrt{1+4a}) \right] \right] U \left(\bar{t} - \frac{\bar{x}}{\kappa} \right) \right\}. \tag{5}
 \end{aligned}$$

From here, at $\bar{x} = \kappa \bar{t}$, we find the temperature at the combustion front

$$T_f - T_0 = (T_s - T_0) \exp \left[-\frac{\kappa \bar{t}}{2} (-1 + \sqrt{1 + 4a}) \right] + \frac{N_0 g}{c_a \sqrt{1 + 4a}} [1 - \exp(-\kappa \bar{t} \sqrt{1 + 4a})]. \quad (6)$$

At $T_s = T_0$ and after a sufficiently long time, we have

$$T_f - T_0 = \frac{N_0 g}{c_a \sqrt{1 + 4a}}. \quad (7)$$

With the temperature measured at the combustion front, we determine from this relation the dimensionless parameter

$$a = \frac{1}{4} \left[\frac{(N_0 g)^2}{c_a^2 (T_f - T_0)^2} - 1 \right]. \quad (8)$$

In order to compare the measured and the calculated temperature distribution in the model, we represent Eq. (5) in dimensional form with $T_s = T_0$:

$$T - T_0 = \frac{N_0 g}{c_a \sqrt{1 + 4a}} \left\{ \exp \left[\frac{1}{2} (x - vt)(c - \sqrt{c^2 + 4\bar{k}}) \right] - \exp \frac{1}{2} [c(x - vt) - (x + vt) \sqrt{c^2 + 4\bar{k}}] - \left[\exp \left[-\frac{1}{2} (vt - x) \times (c - \sqrt{c^2 + 4\bar{k}}) \right] - \exp \left[-\frac{1}{2} (vt - x)(c + \sqrt{c^2 + 4\bar{k}}) \right] \right] U(vt - x) \right\}, \quad (9)$$

where

$$c = c_a \rho_a u / \lambda, \quad \bar{k} = 2k / \lambda R.$$

If the values of parameters c and \bar{k} were considered to be the same in the regions separated by the combustion front, then the calculated and the measured distribution curves would not agree. This suggests that parameters c and \bar{k} have different values in those regions, which follows from the physical nature of the combustion process.

The values of parameters c and \bar{k} before and behind the combustion front will be chosen so as to reconcile as closely as possible the measured temperature values with those calculated according to formula (9). Such a manipulation is entirely permissible, since solution (9) is obtained for each region separately.

The curves of longitudinal temperature distribution in the bed model shown in Fig. 3 have been calculated according to (9) for the instants of time 5.6 h and 6.4 h after the start of combustion, corresponding to the front location at the distances 84 cm and 94 cm respectively. The corresponding measured temperatures are indicated by black and white dots. The matched values of c and \bar{k} were $c = 1/\text{m}$, $\bar{k} = 5/\text{m}^2$ respectively before the front and $c = 3/\text{m}$, $\bar{k} = 200/\text{m}^2$ behind the front. Parameter a , according to (8), was equal to 5. This comparison indicates a satisfactory agreement between tested and calculated values of model temperatures, except near both end sections. An explanation for the discrepancy at the inlet end is that in the theoretical solution the temperature is held equal to the atmospheric temperature, while in the experiment this condition is not observed on account of the reverse heat flow along the metallic shell. An explanation for the discrepancy at the outlet end is that a vapor zone exists before the combustion front in the physical model, while the mathematical model does not account for phase transformations.

An increase in the value of c before the combustion front is due to the higher bulk heat capacity of the heterogeneous convective mass, as a result of the formation of fluid fractions (water, vapor, oil, solvent, etc.). Parameter \bar{k} depends, essentially, on the heat transfer conditions. A fast rise in the heat transfer rate before the combustion front, in addition to being related to the heat losses through the insulation sleeve into the surrounding air, is also related to the heat expenditure on various phase transformations of the hydrocarbons, on vapor generation, on heating up the sandstone matrix, etc.

The temperature distribution pattern in a bed changes considerably during moist and hypermoist combustion. The addition of some quantity of water into the air supply (from 0.0001 to 0.002 m^3/Nm^3)

causes a sharp increase in the bulk heat capacity of the convective mixture, and heat is transferred then to the foremost region of the combustion front. In this way, the heat utilization factor during combustion increases. Solution (9) with a corresponding choice of values for a , c , and \bar{k} renders a description of the temperature field and of the processes involved here.

NOTATION

k	is the heat transfer coefficient;
c_a	is the specific heat of air;
c_s	is the specific heat of sandstone;
λ	is the thermal conductivity;
x	is the distance along the tube;
\bar{x}	is the dimensionless distance;
R	is the radius of the burner tube;
T	is the temperature;
T_0	is the ambient temperature;
T_f	is the temperature at the combustion front;
T_s	is the temperature of injected air;
t	is the time;
\bar{t}	is the dimensionless time;
v	is the velocity of the combustion front;
u	is the air filtration velocity;
M	is the concentration of residual fuel;
γ	is the thermal diffusivity;
\bar{T}	is the dimensionless temperature;
ρ_s	is the density of sandstone;
ρ_a	is the density of air;
N_0	is the concentration of oxygen in air;
g	is the heat of combustion of the residual fuel per 1 kg oxygen;
T_m	is the temperature at the inlet of the preheated model;
b	is the constant;
$\delta(x)$	is the Dirac delta function;
$U(x)$	is the unit function

LITERATURE CITED

1. K. J. Tranter, *Integral Transformations in Mathematical Physics* [Russian translation], Gostekhizdat, Moscow (1956).
2. A. B. Sheinman, G. E. Malofeev, and A. M. Sergeev, *Heat Treatment of a Petroleum Bed during Oil Extraction* [in Russian], Nedra, Moscow (1969).
3. W. L. Penberthy and H. J. Ramey, *J. Soc. Petroleum Eng.*, **6**, No. 2, 183 (1966).